Electronic Structure of U^{3+} in $Cs_3Lu_2Cl_9$ and $Cs_3Y_2I_9$ Single Crystals

Mirosław Karbowiak,*,† Agnieszka Mech,† Janusz Drożdżyński,† Witold Ryba-Romanowski,‡ and Michael F. Reid§

Faculty of Chemistry, University of Wrocław, ul. F. Joliot-Curie 14, 50-383 Wrocław, Poland, W. Trzebiatowski Institute of Low Temperature and Structure Research, Polish Academy of Sciences, P.O. Box 937, 50-937 Wrocław, Poland, and Department of Physics and Astronomy, University of Canterbury, Private Bag 4800, Christchurch 8020, New Zealand

Received: July 5, 2004; In Final Form: October 11, 2004

Low-temperature emission and polarized absorption spectra have been recorded for U^{3+} ions diluted in $Cs_3Lu_2Cl_9$ and $Cs_3Y_2I_9$ host crystals. The experimental crystal-field levels were fitted to 13 parameters of a semiempirical Hamiltonian representing the combined atomic, one-electron crystal field (CF) as well as two-particle correlation crystal-field (CCF) operators. The red shift of the first f−d transitions from ∼14 800 cm^{-1} in the spectrum of U^{3+}:$Cs_3Lu_2Cl_9$ to as low as 11 790 cm^{-1} in that of U^{3+}:$Cs_3Y_2I_9$ has been attributed to an increase in the covalence of the $U^{3+}-X^-$ bonds. Comparison of the differences in the Coulomb repulsion strength between U^{3+} and Er^{3+} ions in $Cs_3Lu_2Cl_9$ and $Cs_3Y_2I_9$ crystals suggests that the 5f electrons of U^{3+} ions are more 3d-like than 4f. The CF splitting of the $^2H_{9/2}$ and $^4F_{5/2}$ multiplets is unexpectedly larger for U^{3+}:$Cs_3Y_2I_9$ than for U^{3+}:$Cs_3Lu_2Cl_9$, which may be viewed as a result of the proximity of f−d states. For a correct description of the energy level structure of the $^2H_{9/2}$ and $^4F_{5/2}$ multiplets, the inclusion of CCF terms in the parametric Hamiltonian has proved to be essential. The larger f−f transition intensities for U^{3+}:$Cs_3Y_2I_9$ were also considered to be a consequence of the red shift of the first f−d states. The inadequacy in determination of the minor atomic parameters (other than parameters for Coulomb and spin−orbit interactions) and the insufficient inclusion of the influence of excited configuration in the applied CF Hamiltonian are assumed to be the main deficiencies preventing a better agreement between the experimental and calculated energies of CF levels.

1. Introduction

In recent years, a number of crystal-field analyses of U^{3+} ions in polycrystalline samples and single host crystals have been reported.[1−5] Since $LaCl_3$ (refs 6 and 7), $LiYF_4$ (ref 8), and Cs_2MYX_6 (where M = Li or Na and X = Cl or Br)[9,10] were the only host crystals in which the uranium ions were located at a site symmetry higher than C_{2v}, we turned our attention toward high-symmetry hosts. Recently, we have completed an analysis on optical spectra and crystal-field (CF) calculations of U^{3+}-doped $CsCdBr_3$ single crystals.[11] The uranium ions incorporated in this host crystal possess C_{3v} site symmetry. However, the C_{3v} crystal field can be described as a superposition of a dominant octahedral and a weaker trigonal part.[12] This is evidenced by a close similarity of the energy level structure of U^{3+}:$CsCdBr_3$ and U^{3+}:Cs_2NaYBr_6 (ref 10) as well as by the presence of Γ_4 and $\Gamma_{5,6}$ levels originating from quadruplet degenerated $\Gamma_8(O_h)$ states as relatively closely positioned doublets. C_{3v} site symmetry, also related to that of O_h but with a larger distortion resulting from a larger contribution of the trigonal part to the CF potential, is observed for the $Cs_3Lu_2X_9$ (X = Cl, Br, or I) type of compounds.

In this paper, the results of our spectroscopic investigations on U^{3+}-doped $Cs_3Lu_2Cl_9$ and $Cs_3Y_2I_9$ single crystals are presented. Due to a similar surrounding of the U^{3+} ions, these host crystals together with those of $CsCdBr_3$ (ref 11) and Cs_2NaYX_6 (X = Cl or Br)[9,10] are suitable for comparison purposes on the influence of the descending site symmetry on the structure of the crystal-field levels. Besides, with the variation of the environment from chloride to iodide ligands, some trends in the energy level structure of the $5f^3$ and $5f^26d^1$ configuration could be investigated. Such a comparison has been so far reported for the U^{3+}:K_2LaX_5 (X = Cl, Br, or I) single crystals only,[13] showing a considerably smaller CF effect exerted by the iodide ligands on the uranium ion and a larger covalency of the U−I bonds due to a larger polarizability. Since the electronic energy level structure and correlation crystal-field effects have been recently studied in detail also for Er^{3+}-doped $Cs_3Lu_2Cl_9$ and $Cs_3Y_2I_9$ single crystals,[14,15] the discussion could be enhanced by a comparison of the obtained results.

2. Experimental Section

The starting materials for the synthesis of the U^{3+}:$Cs_3Lu_2Cl_9$ single crystals were CsCl, $LuCl_3$, and UCl_3. Cesium chloride was prepared by reaction of concentrated HCl on Cs_2CO_3. The obtained CsCl powder was dried and purified by sublimation in a vacuum. $LuCl_3$ was prepared from Lu_2O_3 (99.99%) following the ammonium halide route.[16] For purification, $LuCl_3$ was sublimated in a vacuum and passed through a Bridgman furnace. UCl_3 was prepared by thermal decomposition of $NH_4UCl_4 \cdot 4H_2O$ according to the method reported in ref 17. Due to incongruent melting of $Cs_3Lu_2Cl_9$, a nonstoichiometric mixture of CsCl and a 5% excess of $LuCl_3$ was sealed under vacuum in a silica ampule and passed through a vertical Bridgman furnace. The $Cs_3Lu_2Cl_9$ crystals thus obtained were mixed with UCl_3

* Corresponding author. E-mail: karb@wchuwr.chem.uni.wroc.pl. Phone: +48 71 3757304. Fax: +48 3282348.
† University of Wrocław.
‡ Polish Academy of Sciences.
§ University of Canterbury.

10.1021/jp047047h CCC: $30.25
Published on Web 12/04/2004

(in an ~100:1 ratio) and a 5% excess of $LuCl_3$, and the mixture was again passed through the furnace.

Since $Cs_3Y_2I_9$, in contrast to $Cs_3Lu_2Cl_9$, melts congruently, it could be prepared by reaction of stoichiometric amounts of CsI, I_2, and yttrium powders. The mixture was placed in a silica ampule, sealed under high vacuum, and heated in a furnace for 3 days at 250 °C. The obtained powder was next sublimated under high vacuum, placed in a silica tube, and passed through a Bridgman furnace. The obtained crystals were mixed in an ~100:1 ratio with UI_3 and passed again through the furnace. Uranium triiodide was synthesized by reaction of uranium powder, obtained by decomposition of UH_3, with an excess of iodine. The substrates were placed in a silica tube, sealed under vacuum, and heated in a furnace for 2 days at temperatures being gradually increased from 200 to 350 °C. The obtained crystals were checked for phase purity by X-ray powder diffractometry. The concentration of uranium in both crystals has been determined by inductively coupled plasma (ICP) spectrometry.

For spectroscopic measurements, ~5 × 5 × 1 mm^3 plates were cut from bulk crystals and polished under dry paraffin oil. Optically oriented crystals were mounted in an Oxford Instruments model CF1204 cryostat and cooled to ~7 K. Polarized absorption spectra were recorded in the 3900−30000 cm^{-1} range. Unpolarized luminescence spectra were excited either by an argon ion laser or by a Continuum OPO model Surelite I pumped by the third harmonic of a Nd:YAG laser. The sample luminescence was dispersed by a 1 m double-grating monochromator, detected by a photomultiplier, and analyzed by a Stanford model SRS 250 Boxcar integrator. In the luminescence decay measurements, a Tektronix model TDS 3052 digital oscilloscope has been used.

3. Theory

For the energy level calculations, we have applied the effective operator model.[18,19] The observed energy levels were fitted to the phenomenological Hamiltonian $\hat{H} = \hat{H}_{FI} + \hat{H}_{CF} + \hat{H}_{CCF}$ by simultaneous diagonalization of the free-ion ($\hat{H}_{FI}$) and crystal-field ($\hat{H}_{CF}$ and $\hat{H}_{CCF}$) Hamiltonians. The free-ion Hamiltonian is given by

$$\hat{H}_{FI} = E_{av} + \sum_{k=2,4,6} F^k(nf, nf)\,\hat{f}_k + \zeta_{5f}\hat{A}_{SO} + \alpha\hat{L}(\hat{L}+1) + \beta\hat{G}(G_2) + \gamma\hat{G}(R_7) + \sum_{i=2,3,4,6,7,8} T^i\hat{t}_i + \sum_j M^j\hat{m}_j + \sum_k P^k\hat{p}_k \quad (1)$$

where E_{av} is the spherically symmetric one-electron part of the Hamiltonian, $F^k(nf, nf)$ and ζ_{5f} represent the radial parts of the electrostatic and spin−orbit interactions, and $\hat{f}_k$ and $\hat{A}_{SO}$ are the angular parts of these interactions, respectively. The α, β, and γ parameters are associated with the two-body correction terms. They account for the radial interactions not transforming as $\hat{f}_k$. $\hat{G}(G_2)$ and $\hat{G}(R_7)$ are Casimir operators for the groups G_2 and R_7, respectively, and L is the total orbital angular momentum. The three-particle configuration interaction is expressed by $T^i\hat{t}_i$ (i = 2, 3, 4, 6, 7, or 8), where T^i are parameters and $\hat{t}_i$ are three-particle operators. The electrostatically correlated spin−orbit perturbation is represented by the P^k parameters, and those of the spin−spin and spin−other-orbit relativistic corrections are represented by the M^j parameters. The operators associated with these parameters are designated by $\hat{p}_k$ and $\hat{m}_j$, respectively.

The U^{3+} ions substitute for Lu^{3+} or Y^{3+} in sites of an approximately C_{3v} symmetry. For this symmetry, the crystal-field Hamiltonian can be expressed in terms of phenomenological B_q^k crystal-field parameters and the $\hat{U}_q^k$ unit tensor operators as follows:

$$\hat{H}_{CF} = B_0^2\,\hat{U}_0^2 + B_0^4\,\hat{U}_0^4 + B_3^4(\hat{U}_3^4 - \hat{U}_{-3}^4) + B_0^6\,\hat{U}_0^6 + B_3^6(\hat{U}_3^6 - \hat{U}_{-3}^6) + B_6^6(\hat{U}_6^6 + \hat{U}_{-6}^6) \quad (2)$$

In this study, the unit tensor normalization was chosen for the one-particle crystal-field operators instead of the more usually applied spherical tensor normalization. The parameters in these two different normalizations are related by[20]

$$B_q^k(\text{as a function of } C_q^{(k)}) = (-1)^q(\langle l_f||C^{(k)}||l_f\rangle)^{-1}B_q^k(\text{as a function of } U_q^k) \quad (3)$$

where

$$\langle l_f||C^{(k)}||l_f\rangle = (-1)^{l_f}(2l_f+1)\begin{pmatrix} l_f & k & l_f \\ 0 & 0 & 0\end{pmatrix}$$

The last term of the complete Hamiltonian represents the correlated two-electron crystal-field interactions. Following Reid,[21] the parametrization of these interactions may be written in Judd's notation[22] as a set of G_{iq}^k parameters

$$\hat{H}_{CCF} = \sum_{i,k,q} G_{iq}^k\,\hat{g}_{iq}^{(k)} \quad (4)$$

where k runs through the even integers from 0 to 12, i distinguishes different $\hat{g}_{iq}^{(k)}$ operators with identical k, and q is restricted by the crystal-field symmetry.

Since there are 41 independent correlation crystal-field (CCF) parameters, it was not possible to include all of them in a fit with a set of 57 or 39 experimental data only. However, Li and Reid[23] in an analysis of a number of Nd^{3+}-doped crystals have shown that the inclusion of a few CCF parameters only has markedly improved the fits and could resolve problems with poorly fitted levels by the one-electron crystal-field operator H_{CF}. Parameters showing for the appropriate levels large values of matrix elements have obviously the largest influence on the problematic multiplets. In the present calculations of the U^{3+}-doped title crystals, similarly as in our previous analysis of U^{3+}:$CsCdBr_3$, the most problematic multiplets were $^2H_{9/2}$ and $^4F_{5/2}$ (ref 11) due to a considerable discrepancy between the values of the experimental splitting and those calculated in the one-electron crystal-field model. Besides, the order of some CF energy levels in these multiplets also could not be correctly reproduced. In the case of the $^2H_{9/2}$ and $^4F_{5/2}$ multiplets, the largest matrix element values show the G_{10Aq}^4 and G_{4q}^4 CCF parameters, respectively. Since the q value is for C_{3v} site symmetry restricted to 0 and 3, only four CCF parameters may occur. Hence, the $\hat{H}_{CCF}$ Hamiltonian employing terms connected with those four CCF parameters is defined as

$$\hat{H}_{CCF} = \sum_{q=0,3} G_{10Aq}^4\,\hat{g}_{10Aq}^4 + \sum_{q=0,3} G_{4q}^4\,\hat{g}_{4q}^{(4)} \quad (5)$$

For a further reduction of the number of independent parameters, one may assume an identical q dependence for the CCF and one-electron CF interaction parameters: $G_{10A3}^4 = (B_3^4/B_0^4)\cdot G_{10A0}^4$ and $G_{43}^4 = (B_3^4/B_0^4)\cdot G_{40}^4$. Hence, only two independent CCF parameters remain and were utilized in the fitting procedure according to eq 6:

$$\hat{H}_{CCF} = G_{10A0}^4\left(\hat{g}_{10A0}^{(4)} + \frac{B_3^4}{B_0^4}\hat{g}_{10A3}^{(4)}\right) + G_{40}^4\left(\hat{g}_{40}^{(4)} + \frac{B_3^4}{B_0^4}\hat{g}_{43}^{(4)}\right) \quad (6)$$

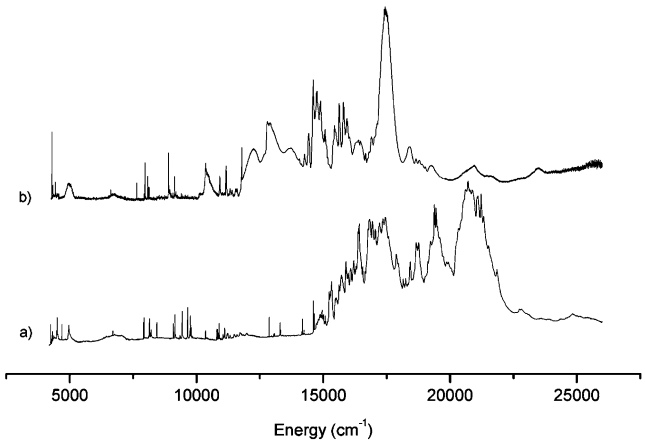

Figure 1. Unpolarized survey absorption spectra measured at 7 K for (0.5%)U^{3+}:$Cs_3Lu_2Cl_9$ (a) and (0.3%)U^{3+}:$Cs_3Y_2I_9$ (b).

In energy level calculations, the complete (364 × 364) $SLJM_J$ matrix was diagonalized. The calculations were performed by applying the f-shell empirical programs[24] and were running on a PC under the Linux Mandrake operating system. The quality of the fits to the above expressions was determined using the root mean square (rms) deviation (in inverted centimeters), defined as

$$\mathrm{rms} = \sum_{i=1}^{n}\left(\frac{(E_{\mathrm{exp}}(i) - E_{\mathrm{calc}}(i))^2}{n-p}\right)^{1/2} \qquad (7)$$

where n is equal to the number of levels and p is the number of parameters that are varied freely. To compare the magnitudes of the total crystal-field strength, the scalar parameter[25]

$$N_{\mathrm{v}} = \left[\sum_{k,q}(B_q^k)^2\frac{4\pi}{(2k+1)}\right]^{1/2} \qquad (8)$$

has been applied.

4. Results

4.1. Absorption and Luminescence Spectra. A survey of the absorption spectra of 0.5% U^{3+}:$Cs_3Lu_2Cl_9$ and 0.3% U^{3+}:$Cs_3Y_2I_9$ at 7 K is shown in Figure 1.

In the spectra, one may distinguish two transition ranges. Parity forbidden, intraconfigurational $5f^3 \rightarrow 5f^3$ transitions were observed in the 4250−15200 cm^{-1} and 4280−11800 cm^{-1} ranges of U^{3+}:$Cs_3Lu_2Cl_9$ and U^{3+}:$Cs_3Y_2I_9$, respectively. Above these ranges, the bands were obscured by very intense and broad parity-allowed $5f^3 \rightarrow 5f^26d^1$ transitions. In the Er^{3+}-doped $Cs_3Lu_2Cl_9$ single crystals, the f−f transitions were strongly polarized, while, for Er^{3+}:$Cs_3Y_2I_9$, the effect of polarization was not clearly observed[14] and it is for U^{3+}:$Cs_3Lu_2Cl_9$ far less pronounced than for the Er^{3+} ions. The π- and σ-polarized ortho-axial absorption spectra of U^{3+}:$Cs_3Lu_2Cl_9$ in the $^4I_{9/2} \rightarrow {}^4I_{13/2}$ and $^4I_{9/2} \rightarrow ({}^2H_{9/2} + {}^4F_{5/2})$ transition ranges are presented in Figures 2 and 3, respectively. A slightly more distinct polarization effect was observed in the π- and σ-polarized absorption spectra of U^{3+}:$Cs_3Y_2I_9$. An α-polarized axial absorption spectrum of this crystal has been also recorded. Representative examples are presented in Figures 4 and 5.

Figure 6 presents luminescence spectra of the U^3:$Cs_3Lu_2Cl_9$ and U^3:$Cs_3Y_2I_9$ single crystals. The observed bands correspond to $^4G_{7/2} \rightarrow {}^4I_{9/2}$ and $^4G_{5/2} \rightarrow {}^4I_{9/2}$ transitions in the chloride and iodide crystal, respectively, and were recorded while exciting the broad f−d transition at 18 797 cm^{-1} (532 nm). For both crystals, the observed emission signal was relatively weak. Nevertheless, for U^{3+}:$Cs_3Y_2I_9$, the lines corresponding to transitions from the $^4G_{5/2}$ multiplet to the five Stark components of the $^4I_{9/2}$ ground multiplet may be easily identified and are indicated by arrows in Figure 6a. The obtained energies of the CF components of the $^4I_{9/2}$ multiplet are equal to 0, 23, 133, 354, and 457 cm^{-1}. For U^3:$Cs_3Lu_2Cl_9$, the assignment is somewhat more complicated, since, in the 12 800 cm^{-1} energy range, where a transition to the second component of the ground multiplet is expected, additional lines, most probably of vibronic origin, were observed. A helpful hint is given by the absorption spectrum recorded at 100 K, where hot bands of transitions to the main lines of the $^2H_{9/2}$ and $^4I_{13/2}$ multiplets were shifted by ∼50 cm^{-1}. Hence, the line observed in the emission spectrum at 12 823 cm^{-1}, spaced from the highest-energy line (at 12 868 cm^{-1}) by 45 cm^{-1}, should correspond to transitions to the second component of the $^4I_{9/2}$ level. This line and the four other lines assigned as zero-phonon lines are indicated by arrows in Figure 6b. The obtained energies of the Stark components of the $^4I_{9/2}$

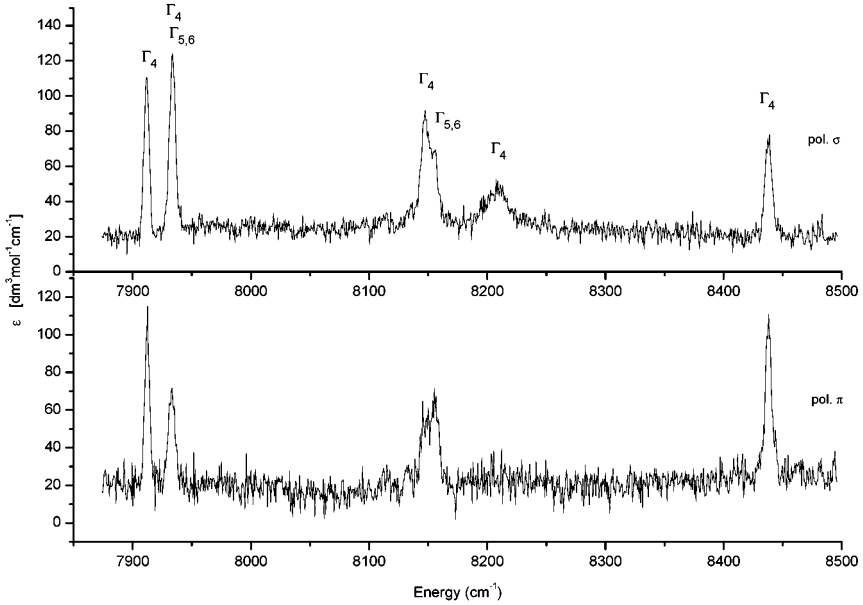

Figure 2. π- and σ-polarized ortho-axial absorption spectrum of U^{3+}:$Cs_3Lu_2Cl_9$ at 7 K in the $^4I_{9/2} \rightarrow {}^4I_{13/2}$ transition range. The assignment to irreducible representations was based on the polarization dependence of the crystal-field transitions and a comparison with the polarized spectra of U^{3+}:$Cs_3Y_2I_9$ and U^{3+}:$CsCdBr_3$ single crystals; see text for details.

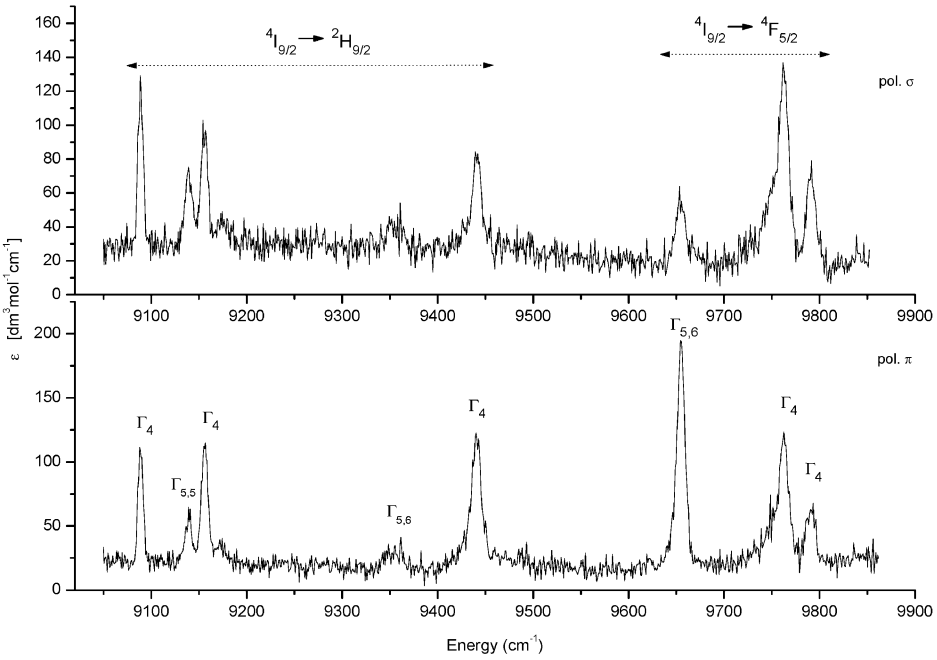

Figure 3. π- and σ-polarized ortho-axial absorption spectra of U^{3+}:$Cs_3Lu_2Cl_9$ at 7 K in the $^4I_{9/2} \rightarrow {}^2H_{9/2}$ and $^4I_{9/2} \rightarrow {}^4F_{5/2}$ transition range. The assignment to irreducible representations was based on the polarization dependence of the crystal-field transitions and a comparison with the spectra of U^{3+}:$Cs_3Y_2I_9$ and U^{3+}:$CsCdBr_3$ single crystals; see text for details.

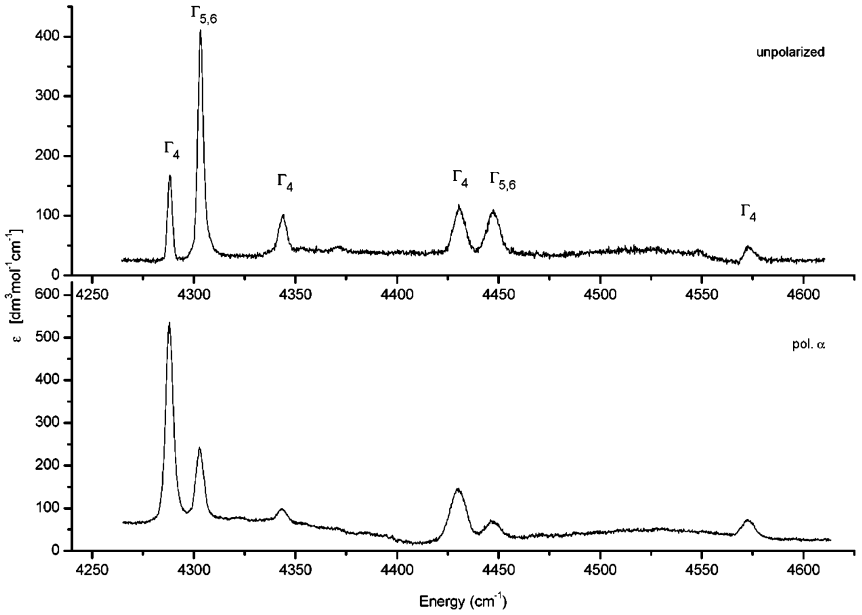

Figure 4. α-Polarized axial absorption spectra of U^{3+}:$Cs_3Y_2I_9$ at 7 K in the $^4I_{9/2} \rightarrow {}^4I_{11/2}$ transition range. The assignment to irreducible representations was based on the polarization dependence of the crystal-field transitions and a comparison with the spectra of U^{3+}:$CsCdBr_3$ single crystals; see text for details.

ground multiplet of U^{3+}:$Cs_3Lu_2Cl_9$ are equal to 0, 44, 179, 319, and 599 cm^{-1}. Figure 7 presents the fluorescence transient observed for the $^4G_{5/2} \rightarrow {}^4I_{9/2}$ emission transition (10 345 cm^{-1}) of U^{3+}:$Cs_3Y_2I_9$. The decay curve was fitted with a biexponential function, and time constants of 0.6 and 5.2 μs were determined. For U^{3+}:K_2LaI_5, a lifetime of 19 μs has been reported for emission from the $^4G_{5/2}$ level at 14 K.[13] One may assume, therefore, that the value 5.2 μs corresponds to the lifetime of the $^4G_{5/2}$ emitting level of U^{3+} in $Cs_3Y_2I_9$, but the origin of the short, 0.6 μs component is not clear. The lifetime of U^{3+} in $Cs_3Y_2I_9$ is a factor of 4 shorter than that determined for U^{3+}:K_2LaI_5, which primarily results from the shorter $U^{3+}-I^-$ distances, which lead to a stronger CF and larger electron−phonon coupling of the U^{3+} ions in $Cs_3Y_2I_9$. Unfortunately, in the case of U^{3+}:$Cs_3Lu_2Cl_9$, the decay time was very short, comparable to a 9 ns duration of the laser pulse, making an accurate recording not possible.

4.2. Energy Level Calculations. From the analysis of the absorption and emission spectra, 57 and 39 energy levels were assigned for U^{3+}:$Cs_3Lu_2Cl_9$ and U^{3+}:$Cs_3Y_2I_9$, respectively (Tables 1 and 2). The energy range available for the analysis is limited to 0−15 200 cm^{-1} for the chloride crystal and to 0−11 800 cm^{-1} for the iodide crystal, which spans 11 and 9 of the lowest-energy SLJ multiplet manifolds of the $5f^3(U^{3+})$ electronic configuration of U^{3+}:$Cs_3Lu_2Cl_9$ and U^{3+}:$Cs_3Y_2I_9$, respectively. Above these energy ranges, the f−f transitions could not be identified due to a strong interference with the f−d bands.

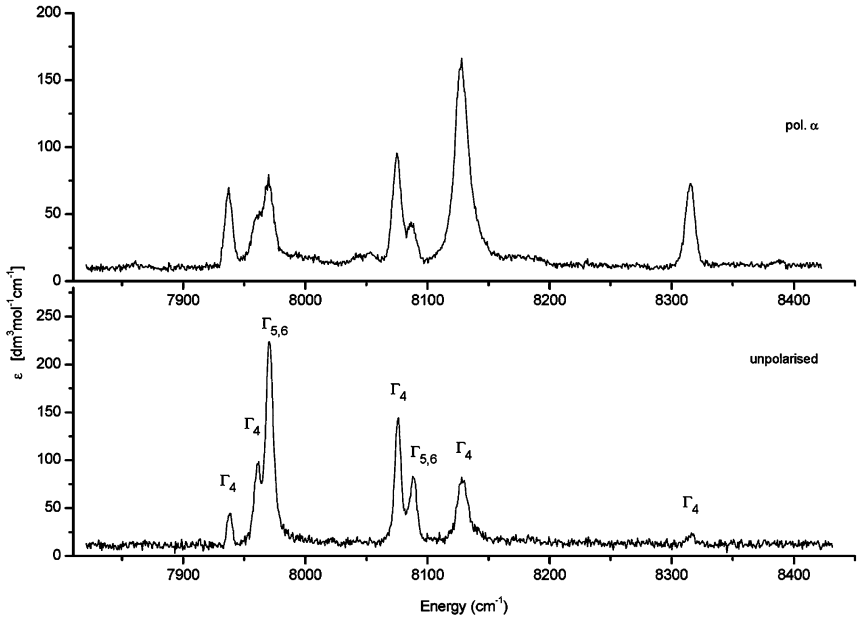

Figure 5. α-Polarized axial absorption spectra of U^{3+}:$Cs_3Y_2I_9$ at 7 K in the $^4I_{9/2} \rightarrow {}^4I_{13/2}$ transition range. The assignment to irreducible representations was based on the polarization dependence of the crystal-field transitions and a comparison with the spectra of U^{3+}:$CsCdBr_3$ single crystals; see text for details.

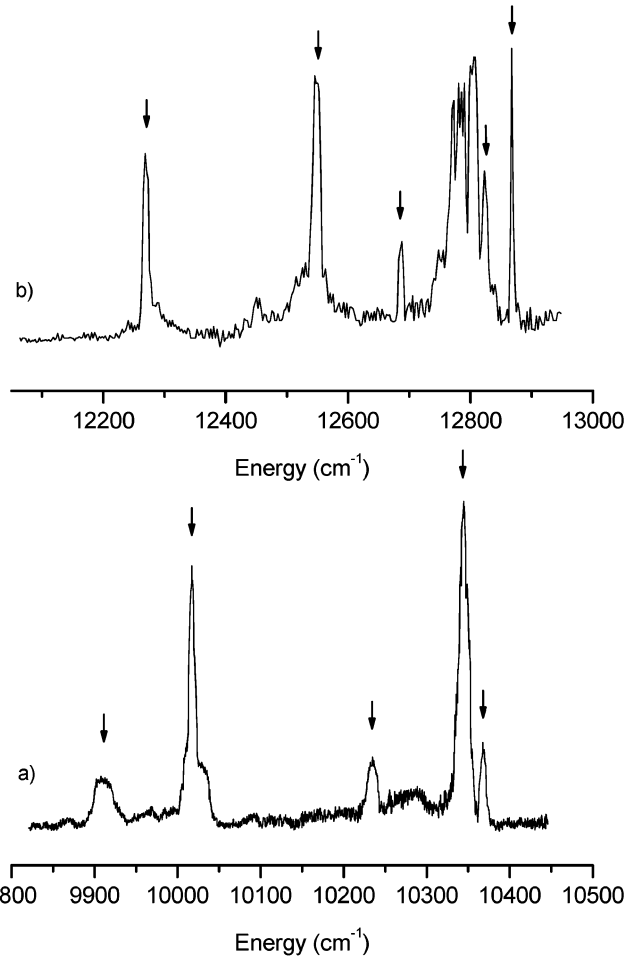

Figure 6. The 4.2 K emission spectra showing the $^4G_{7/2} \rightarrow {}^4I_{9/2}$ transitions of U^{3+}:$Cs_3Lu_2Cl_9$ (a) and the $^4G_{5/2} \rightarrow {}^4I_{9/2}$ transitions of U^{3+}:$Cs_3Y_2I_9$ (b), recorded after 18 797 cm^{-1} (532 nm) excitation, which corresponds to the broad $5f^3 \rightarrow 5f^26d^1$ absorption transitions of U^{3+}. The zero-phonon lines are marked by arrows.

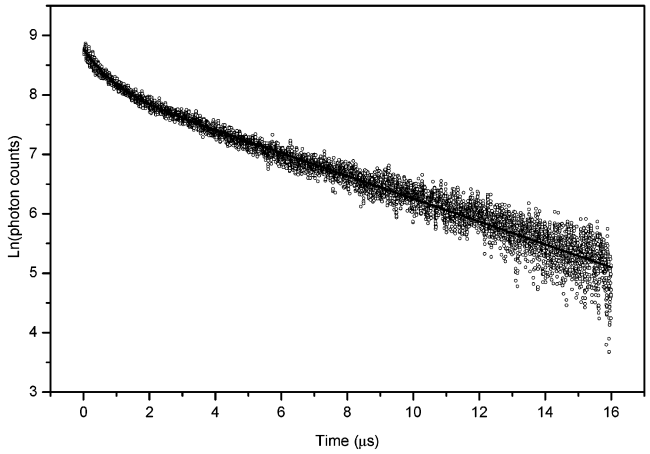

Figure 7. Fluorescence transient in a semilogarithmic scale observed at 4.2 K for the $^4G_{5/2} \rightarrow {}^4I_{9/2}$ emission transition (10 345 cm^{-1}) of U^{3+}:$Cs_3Y_2I_9$.

The experimental energy levels were fitted to the parameters of a phenomenological Hamiltonian (eqs 1−6). The "free-ion" parameters obtained for U^{3+}:$LaCl_3$ (ref 7) and twice as large values of the crystal-field parameters obtained for Er^{3+}:$Cs_3Lu_2Cl_9$ and Er^{3+}:$Cs_3Y_2I_9$[14] have been applied as starting points. The Slater (F^k) and spin−orbit coupling (ζ_{5f}) parameters as well as six CF and two CCF crystal-field parameters were allowed to freely vary. The remaining free-ion parameters were constantly fixed at their starting values.

The calculations were done for the complete $5f^3$ configuration leading to a (364 × 364) energy matrix and were performed for the one-electron crystal-field model and for the extended model, which encompasses the four selected two-particle correlation crystal-field (CCF) operators. In the one-electron parametrization scheme, we obtained a standard deviation of $\sigma = 50$ cm^{-1} for 57 fitted levels of U^{3+}:$Cs_3Lu_2Cl_9$. After inclusion of the CCF terms, the error decreased to 35 cm^{-1}. For the more limited experimental data set of 39 energy levels of U^{3+}:$Cs_3Y_2I_9$, the deviations were equal to 48 and 37 cm^{-1} for the CF and CCF models, respectively. The experimental and calculated energy level values are listed in Tables 1 and 2 for U^{3+}:$Cs_3Lu_2Cl_9$ and U^{3+}:$Cs_3Y_2I_9$, respectively. The best sets of the parameters derived in the fitting procedure are given in Table 3.

TABLE 1: Calculated and Experimental Energy Levels of U^{3+} in $Cs_3Lu_2Cl_9$ Single Crystals

		energy (cm^{-1})				
			CF[a]		CCF[b]	
multiplet	irrep	E_{exp}	E_{calc}[c]	$E_{exp} - E_{calc}$	E_{calc}[c]	$E_{exp} - E_{calc}$
$^4I_{9/2}$	$\Gamma_{5,6}$	0	60*	−60	22*	−22
	Γ_4	44	9*	35	−5*	49
	Γ_4	179	158	21	127	52
	Γ_4	319	328	−9	350	−31
	$\Gamma_{5,6}$	599	522	77	580	19
$^4I_{11/2}$	Γ_4	4252	4250	2	4241	11
	$\Gamma_{5,6}$	4291	4294	−3	4285	5
	Γ_4	4313	4309	4	4301	12
	Γ_4	4484	4490	−7	4486	−2
	$\Gamma_{5,6}$	4509	4523	−14	4525	−16
	Γ_4	4695	4696	−1	4714	−19
$^4F_{3/2}$	$\Gamma_{5,6}$	6697	6752	−56	6739	−42
	Γ_4	6944	6928	16	6943	1
$^4I_{13/2}$	Γ_4	7912	7897	15	7897	15
	Γ_4	7936	7919*	17	7919*	17
	$\Gamma_{5,6}$	7936	7918*	18	7916*	20
	Γ_4	8148	8143	5	8130	18
	$\Gamma_{5,6}$	8155	8169	−14	8150	5
	Γ_4	8215	8253	−39	8259	−44
	Γ_4	8439	8461	−22	8470	31
$^2H_{9/2}$	Γ_4	9090	9161*	−71	9082	8
	$\Gamma_{5,6}$	9139	9032*	107	9167	−28
	Γ_4	9157	9238	−80	9185	−27
	$\Gamma_{5,6}$	9351	9389*	−38	9363	−12
	Γ_4	9443	9385*	57	9417	26
$^4F_{5/2}$	$\Gamma_{5,6}$	9656	9720*	−64	9704*	−48
	Γ_4	9764	9668*	96	9672*	91
	Γ_4	9794	9781	12	9773	21
$^4G_{5/2}$ +	Γ_4	10 356	10 376	−21	10 399	−43
$^4S_{3/2}$ +	$\Gamma_{5,6}$	10 800	10 760	40	10 804	−4
$^4F_{7/2}$ +	Γ_4	10 835	10 848	−14	10 893	−58
$^4I_{15/2}$	Γ_4	10 890	10 918	−28	10 928	−39
	Γ_4	11 050	11 069	−19	11 071	−22
	$\Gamma_{5,6}$	11 110	11 090	20	11 098	12
	$\Gamma_{5,6}$	11 212	11 254*	−42	11 229*	−17
	Γ_4	11 231	11 192*	40	11 215*	16
	Γ_4		11 287		11 270	
	Γ_4	11 328	11 310	18	11 324	4
	$\Gamma_{5,6}$	11 450	11 467	−17	11 446	4
	Γ_4	11 487	11 542	−56	11 526	−39
	$\Gamma_{5,6}$	11 585	11 623*	−38	11 602	−17
	Γ_4	11 601	11 601*	0	11 609	−8
	Γ_4	11 721	11 687	34	11 657	64
	Γ_4	11 769	11 764	5	11 792	−23
	$\Gamma_{5,6}$	11 981	11 993	−12	12 005	−24
$^4G_{7/2}$	Γ_4	12868	12900	−32	12870	−3
	Γ_4	13043	13036	7	13043	12
	$\Gamma_{5,6}$	13074	13094	−20	13074	10
	Γ_4	13302	13239	62	13302	51
$^4F_{9/2}$	Γ_4	14158	14164	−6	14130	28
	$\Gamma_{5,6}$	14178	14182	−4	14216	−38
	Γ_4	14237	14240	−3	14242	−5
	$\Gamma_{5,6}$	14604	14553	60	14560	44
	Γ_4	14635	14581	54	14592	43
$^2H2_{11/2}$	$\Gamma_{5,6}$	14953	15060*	−107	14987	−34
	Γ_4	15005	14952*	53	14990	15
	Γ_4	15074	15020*	53	15036	38
	Γ_4	15098	15080	18	15109	−11
	Γ_4	15149	15173	−24	15137	12
	$\Gamma_{5,6}$		15196		15165	

[a] One-electron crystal-field (CF) analysis. [b] Two-particle correlation crystal-field (CCF) analysis. [c] Calculated Stark components denoted by an asterisk have been reordered to correspond to the experimental assignment.

TABLE 2: Calculated and Experimental Energy Levels of U^{3+} in $Cs_3Y_2I_9$ Single Crystals

		energy (cm^{-1})				
			CF[a]		CCF[b]	
multiplet	irrep	E_{exp}	E_{calc}[c]	$E_{exp} - E_{calc}$	E_{calc}[c]	$E_{exp} - E_{calc}$
$^4I_{9/2}$	$\Gamma_{5,6}$	0	57*	−57	30*	−30
	Γ_4	23	−14*	36	−11*	34
	Γ_4	133	175	−42	160	−27
	Γ_4	354	294	60	294	60
	$\Gamma_{5,6}$	457	442	15	461	−4
$^4I_{11/2}$	Γ_4	4287	4283	4	4270	17
	$\Gamma_{5,6}$	4303	4289	14	4296	7
	Γ_4	4344	4317	27	4325	18
	Γ_4	4431	4450	−19	4433	−3
	$\Gamma_{5,6}$	4447	4473	−26	4474	−26
	Γ_4	4572	4559	13	4584	−12
$^4F_{3/2}$	$\Gamma_{5,6}$	6623	6659	−36	6730	−7
	Γ_4	6756	6719	37	6749	7
$^4I_{13/2}$	Γ_4	7936	7913	23	7931	5
	Γ_4	7960	7950*	10	7977*	−17
	$\Gamma_{5,6}$	7970	7938*	32	7951*	19
	Γ_4	8077	8103	−26	8085	−8
	$\Gamma_{5,6}$	8088	8141	−53	8120	−33
	Γ_4	8129	8180	−51	8194	−65
	Γ_4	8316	8298	18	8312	4
$^2H_{9/2}$	Γ_4	9068	9166*	−98	9082	−15
	$\Gamma_{5,6}$	9133	9111*	22	9220*	−87
	Γ_4	9184	9254	−70	9195*	−11
	$\Gamma_{5,6}$	9401	9366	35	9351	50
	Γ_4	9452	9373	79	9431	21
$^4F_{5/2}$	$\Gamma_{5,6}$	9507	9558	−51	9523	−16
	Γ_4	9557	9575	−18	9536	21
	Γ_4	9666	9616	50	9647	19
$^4G_{5/2}$ +	Γ_4	10 368	10 384	−16	10 385	−17
$^4S_{3/2}$ +	$\Gamma_{5,6}$		10 719		10 760	
$^4F_{7/2}$ +	Γ_4	10 798	10 726	72	10 792	6
$^4I_{15/2}$	Γ_4		10 869		10 870	
	$\Gamma_{5,6}$	10 916	10 964	−48	10 934	−18
	Γ_4	11 023	10 996	27	11 022	1
	Γ_4	11 104	11 121*	−17	11 114*	−10
	$\Gamma_{5,6}$	11 172	11 109*	63	11 087*	85
	Γ_4		11 177		11 200	
	Γ_4		11 216		11 223	
	$\Gamma_{5,6}$	11 332	11 324	8	11 329	3
	Γ_4	11 401	11 367	34	11 396	5
	Γ_4		11 495		11 497	
	$\Gamma_{5,6}$	11 541	11 558	−17	11 514	27
	Γ_4	11 597	11 599	−2	11 581	16
	Γ_4		11 697		11 679	
	$\Gamma_{5,6}$	11 786	11 815	−29	11 799	−13

[a] One-electron crystal-field (CF) analysis. [b] Two-particle correlation crystal-field (CCF) analysis. [c] Calculated Stark components denoted by an asterisk have been reordered to correspond to the experimental assignment.

5. Discussion

5.1. Selection Rules and Irreducible Representation Assignment. $Cs_3Lu_2Cl_9$ crystallizes in the rhombohedral space group $R\bar{3}c$ (ref 26), while $Cs_3Y_2I_9$ in the hexagonal space group $P6_3/mmc$.[27] In these host crystals, the U^{3+} ions substitute for Lu^{3+} or Y^{3+}. The characteristic feature of the structures is $[M_2X_9]^{3-}$ dimers formed by two trigonally distorted, face-sharing $[MX_6]^{3-}$ octahedra. The hexagonal c axes of the crystals coincide with the trigonal axis of the dimer. For $Cs_3Lu_2Cl_9$, the $Lu^{3+}-Cl^-$ bond lengths for the bridging and terminal Cl^- ions are different, equal to 2.658 and 2.461 Å, respectively, and there is a small twist of 1.0° between the terminal and bridging $Lu^{3+}-Cl^-$ bonds. Hence, the real site symmetry of U^{3+} ions in $Cs_3Lu_2Cl_9$ is C_3. In the $Cs_3Y_2I_9$ crystal, the room-temperature site symmetry of the central metal ion is exactly C_{3v}. At 7 K, the actual site symmetry is lowered to C_s due to a reported[27] phase transition at low temperatures. However, since the deviation from C_{3v} symmetry is relatively small, in our CF calculations we have assumed for both crystals the idealized C_{3v} symmetry.

TABLE 3: Hamiltonian Parameters Obtained from Crystal-Field (CF) and Correlation Crystal-Field (CCF) Analysis of U^{3+}:$Cs_3Lu_2Cl_9$ and U^{3+}:$Cs_3Y_2I_9$ (All Values Are in cm^{-1}, except for *n*, Which Is the Number of Assigned Energy Levels Included in the Parametric Data Fits)

	U^{3+}:$Cs_3Lu_2Cl_9$		U^{3+}:$Cs_3Y_2I_9$	
parameter[a]	CF[b]	CCF[b]	CF[b]	CCF[b]
E_{av}	18 996(34)	18 995(26)	18 769(49)	18 793(39)
F^2	37 257(107)	37 186(81)	36 162(136)	36 310(106)
F^4	29 794(130)	30 044(99)	30 601(137)	30 560(109)
F^6	18 947(135)	18 862(102)	18 182(184)	18 486(147)
ζ	1589(13)	1588(10)	1584(15)	1587(12)
B^2_0	1345(97)	1556(69)	275(126)	992(91)
B^4_0	−2806(104)	−2438(79)	−1970(121)	−1351(96)
B^4_3	2145(86)	1959(64)	1439(101)	1337(77)
B^6_0	−91(113)	−271(82)	448(132)	−170(109)
B^6_3	−1106(95)	−1285(92)	−1031(109)	−974(91)
B^6_6	858(102)	706(75)	1190(104)	995(84)
G^4_{10A0}[c]		3242(114)		3233(139)
G^4_{40}[c]		1475(132)		2169(150)
n	57	57	39	39
σ[d]	50	35	48	37

[a] The atomic parameters of the Hamiltonian (eq 1) not listed in this column were kept during the fitting procedure at constant values obtained earlier for U^{3+}:$LaCl_3$ (ref 7) (all values in cm^{-1}): $\alpha = 31.0$, $\beta = -886$, $\gamma = 1928$, $T^2 = 388$, $T^3 = 39$, $T^4 = 154$, $T^6 = -233$, $T^7 = 401$, $T^8 = 300$, $M^0 = 0.672$, $M^2 = 0.376$, $M^4 = 0.255$, $P^2 = 1491.0$, $P^4 = 1118$, $P^6 = 746$. [b] The numbers in parentheses indicate errors in determination of the parameter values. [c] The ratios $G^4_{10A3} = aG^4_{10A0}$ and $G^4_{43} = aG^4_{40}$ were used, with *a* values equal to −0.765 and −0.730 for U^{3+}:$Cs_3Lu_2Cl_9$ and U^{3+}:$Cs_3Y_2I_9$, respectively. [d] rms standard deviation, defined by eq 7.

TABLE 4: Electric-Dipole Selection Rules for f^n Ions (*n* odd) at C_{3v} Symmetry Sites

state	Γ_4	$\Gamma_{5,6}$
Γ_4	σ,π	σ
$\Gamma_{5,6}$	σ	π

Calculations performed for the real C_3 or C_s symmetry would lead to a different number of CF parameters and make a direct comparison impossible. Moreover, for C_{3v} symmetry, there are six CF parameters, while, for C_3 or C_s symmetry, the number of parameters increases to 9 or 15, respectively, which in light of the limited number of experimental data would make computational problems hardly tractable. Because, the idealized C_{3v} symmetry has been assumed also for Er^{3+}:$Cs_3M_2X_9$ (ref 14), a comparison of the CF affecting the U^{3+} and Er^{3+} ions is possible and was one of the aims of this paper.

In all transition regions examined in the present study, the line intensities are dominated by electric-dipole contributions.[6,28] The energy levels of the $5f^3$ electronic configuration are Kramer's doublets and may be classified as having either Γ_4 or $\Gamma_{5,6}$ symmetry in the C_{3v} double-rotation group. The electric-dipole selection rules for C_{3v} symmetry are given in Table 4.

In the case of U^{3+}:$Cs_3Lu_2Cl_9$ single crystals, the polarization effect of absorption transitions was not very pronounced. In most spectral regions, this effect was more distinct for the U^{3+}:$Cs_3Y_2I_9$ crystals. Since both crystals exhibit a similar surrounding of U^{3+} ions, we have assumed within a given multiplet the same sequence of CF levels (irrep). Moreover, in the assignment of irrep to the energy levels, we took advantage of our earlier analyses of U^{3+}:Cs_2NaYX_6 (X = Cl or Br)[9,10] and U^{3+}:$CsCdBr_3$ (ref 11) single crystals. In the Cs_2NaYX_6 crystals, the U^{3+} ions are located in a pure O_h site, while the C_{3v} crystal field affecting U^{3+} ions in $CsCdBr_3$, $Cs_2Lu_2Cl_9$, and $Cs_2Y_2I_9$ single crystals may be described as a superposition of a dominant octahedral part and a weaker trigonal part. Under O_h symmetry, the $5f^3$ configuration splits into Γ_6 and Γ_7 doubly degenerate states and quartet states of Γ_8 symmetry.

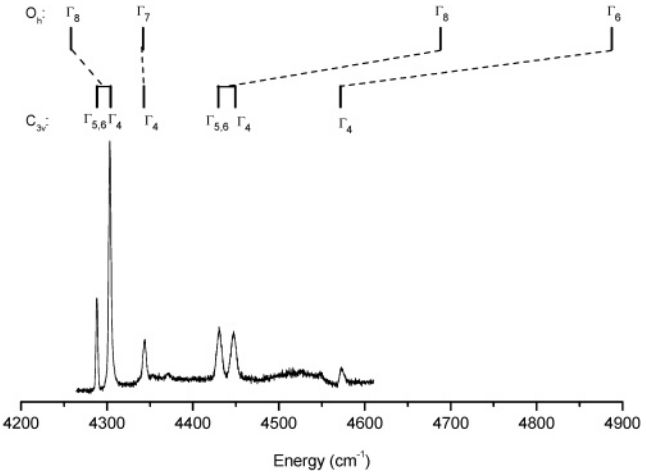

Figure 8. Unpolarized absorption spectrum of U^{3+}:$Cs_3Y_2I_9$ crystals at 7 K in the $^4I_{9/2} \rightarrow {}^4I_{11/2}$ transition range. In the upper part of the figure are schematically marked crystal-field levels of $U^{3+}(O_h)$:Cs_2NaYCl_6 (ref 9).

A weak trigonal (C_{3v}) distortion results in the conversion of the Γ_6 (O_h) and Γ_7 (O_h) states into Γ_4 (C_{3v}) and the splitting of the $\Gamma_8(O_h)$ states into two doublets, Γ_4 (C_{3v}) and $\Gamma_{5,6}$ (C_{3v}). Hence, one should observe in the absorption spectra of U^{3+} ions in the title crystals two closely placed lines, due to transitions to levels arising from the Γ_8 cubic quartet, split by the weak trigonal crystal field. This statement is illustrated in Figure 8 by the $^4I_{9/2} \rightarrow {}^4I_{11/2}$ transitions of U^{3+} in the $Cs_3Y_2I_9$ single crystal. The CF levels of $U^{3+}(O_h)$:Cs_2NaYCl_6 are also schematically indicated in this figure. In an octahedral environment, the following sequence of the U^{3+} CF levels has been determined:[9] $\Gamma_8(O_h)$ (4257 cm^{-1}), $\Gamma_7(O_h)$ (4341 cm^{-1}), $\Gamma_8(O_h)$ (4687 cm^{-1}), and $\Gamma_6(O_h)$ (4877 cm^{-1}). In a crystal field of C_{3v} symmetry, the degenerate quartet $\Gamma_8(O_h)$ splits into $\Gamma_{5,6}(C_{3v})$ and $\Gamma_4(C_{3v})$ components. Obviously, this argumentation may be useful only when the separation between neighboring crystal-field levels in the O_h symmetry is larger than the CF splitting of the Γ_8 states (i.e., the separation between the $\Gamma_{5,6}(C_{3v})$ and $\Gamma_4(C_{3v})$ components) resulting from the trigonal distortion, and the "doublet" components do not overlap with other CF levels. In the $CsCdBr_3$ crystals, the site symmetry of U^{3+} ions located in the principal site, attributed to a symmetric dimer center, is C_{3v} (ref 11), the same as that for the title crystals. Except for the shift of the multiplet baricenters, the structure of the energy levels is very similar to that observed in the $Cs_3Lu_2Cl_9$ and $Cs_3Y_2I_9$ crystals, which is well illustrated in Figure 9. For U^{3+}:$CsCdBr_3$, the polarization selection rules are quite effectively operating.[11] Since in other spectral regions the energy level structure of U^{3+} in the $Cs_3Lu_2Cl_9$ and $Cs_3Y_2I_9$ single crystals should be also very similar to that in $CsCdBr_3$, one may resort to these results in cases when the assignment of the irreducible representations for U^{3+}:$Cs_3Lu_2Cl_9$ and U^{3+}:$Cs_3Y_2I_9$ is ambiguous. A moderate polarization effect observed for U^{3+}:$Cs_3Lu_2Cl_9$ may result from a relatively large (19%) difference in the ionic radius of Lu^{3+} (0.861 Å) and U^{3+} (1.025 Å) which in the process of incorporation of the larger U^{3+} ions could cause local distortions and a larger deviation from the idealized C_{3v} symmetry. The absorption transitions in Er^{3+}:$Cs_3Lu_2Cl_9$ were better polarized due to the similar ionic radii of Er^{3+} (0.890 Å) and Lu^{3+}.

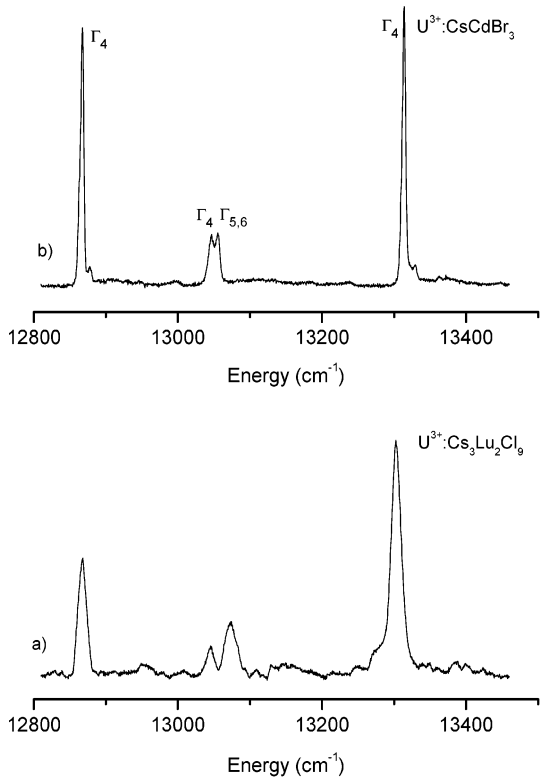

Figure 9. Unpolarized absorption spectra of U^{3+}:$Cs_3Lu_2Cl_9$ (a) and U^{3+}:$CsCdBr_3$ (ref 11) (b) at 7 K in the $^4I_{9/2} \rightarrow {}^4G_{7/2}$ transition range.

Since the fluorescence spectra were recorded with unpolarized light, no assignments of the irreducible representations of the Stark components of the $^4I_{9/2}$ ground multiplet could be directly obtained from experimental data. However, at 7 K, the absorption transitions originate exclusively from the lowest crystal-field level of the $^4I_{9/2}$ state. If one would assume that the ground level is of Γ_4 symmetry, the transitions to the excited Γ_4 levels should be observed as well in σ- and π-polarization, while those to the $\Gamma_{5,6}$ levels in σ-polarization only (Table 4). In the investigated absorption spectra, the intensity of some lines decreases in π-polarization, but some others exhibit considerably lower intensity in the σ-polarized spectra (Figures 2 and 3). Since transitions from the initial $\Gamma_{5,6}$ level to the final Γ_4 or $\Gamma_{5,6}$ levels are allowed in σ- or π-polarization, respectively, the lowest crystal-field component should be assigned as $\Gamma_{5,6}$. This conclusion is supported by an analysis of the axial spectra (Figures 4 and 5), where for some lines one observes distinct intensity changes, while for the initial level of Γ_4 symmetry the α-polarization would not differentiate between transition to the final levels of Γ_4 and $\Gamma_{5,6}$ symmetry. Moreover, the reported $\Gamma_{5,6}$ assignment of the ground state for the Er^{3+}:$Cs_3Lu_2Cl_9$ (ref 14) and U^{3+}:$CsCdBr_3$ single crystals[11] is with this statement also in accordance.

The assignment of the remaining components of the $^4I_{9/2}$ ground multiplet has been achieved by a comparison with the low-temperature absorption spectra of the U^{3+}:$Cs_3Lu_2Cl_9$, U^{3+}:$Cs_3Y_2I_9$, and U^{3+}:Cs_2NaYX_6 (X = Cl or Br)[9,10] single crystals. Under O_h symmetry, the $^4I_{9/2}$ ground multiplet splits into two Γ_8 levels and one Γ_6 level. In the Cs_2NaYCl_6 host crystal, the order of these levels is Γ_8 (0 cm^{-1}), Γ_6 (117 cm^{-1}), and Γ_8 (626 cm^{-1}). In C_{3v} symmetry, the degenerate $\Gamma_8(O_h)$ quartet splits into the $\Gamma_4(C_{3v})$ and $\Gamma_{5,6}(C_{3v})$ components. Thus, the two closely spaced levels of U^{3+}:$Cs_3Lu_2Cl_9$ at 0 and 44 cm^{-1} should originate from the $\Gamma_8(O_h)$ level split by the trigonal crystal field. Since, the lowest Stark component has been assigned as $\Gamma_{5,6}$, that at 44 cm^{-1} ought to be assigned as Γ_4. The next one at 179 cm^{-1} corresponds to Γ_6 in O_h symmetry and is therefore assigned as Γ_4. The following two levels located at 319 and 599 cm^{-1} should arise from the Γ_8 cubic quadruplet and have been assigned as Γ_4 and $\Gamma_{5,6}$. Since, on the grounds of the experimental data, it was not possible to make a distinction between the two possible symmetries, the levels were assigned on the basis of the results obtained from crystal-field calculations.

5.2. Comparison of the Energy Level Structure and Line Intensities. The similarity between the site symmetries of U^{3+} ions in both crystals makes possible investigations on the influence of the change of the type of ligands on the energy level structure. Strong and broad bands, due to the Laporte-allowed f−d transitions, have been observed in the iodide and chloride crystals at ∼11 800 and 14 500 cm^{-1}, respectively. For the U^{3+}:$Cs_3Lu_2Cl_9$ crystal, the zero-phonon lines and vibronic transitions form a fine structure superimposed on the broad f−d bands. For U^{3+}:$Cs_3Y_2I_9$, the f−d transitions appear at exceptionally low energy. Moreover, two unstructured bands are observed at 11 800−14 200 and 16 800−18 500 cm^{-1}. The absence of a fine structure in the transitions to higher-energy $4f^{N-1}5d$ states has been observed for lanthanide ions in fluoride hosts[29] and was explained by assuming that these high-energy levels are positioned in the conduction band of the host lattice. However, this explanation is unlikely for U^{3+}:$Cs_3Y_2I_9$, where unstructured bands are positioned at relatively low energy.

The octahedral (O_h) CF splits the $6d^1$ configuration into a lower t_{2g} state and an upper e_g state. For the U^{3+} ions in the chloride environment, the CF splitting (10*Dq*) of the $5f^26d^1$ configuration is larger than 20 000 cm^{-1} (ref 30). The spin−orbit coupling of the 6d electrons removes the triply degeneracy of t_{2g} and splits this level into the Γ_{8g} degenerate quartet and a higher-lying Γ_{7g} Kramer doublet. The spin−orbit splitting amounts to ∼3000 cm^{-1} and is much smaller than the splitting that results from the CF interactions.[30] For the $5f^26d^1$ excited configuration, the coupling of these 6d states (resulting from CF and spin−orbit interactions) with the $5f^2$ core leads to a number of levels, which together with the vibronic lines form a rich fine structure observed in the f−d spectra. In addition, the Γ_{8g} state is further split by the trigonal distortion of the CF, which leads to a complex energy level structure and makes a detailed assignment of the lines observed in the f−d transition range impossible. Thus, one can state only that the lines observed for U^{3+}:$Cs_3Lu_2Cl_9$ and U^{3+}:$Cs_3Y_2I_9$ in the 14 000−22 500 and 11 800−20 000 cm^{-1} ranges, respectively, are due to transitions from the ground $^4I_{9/2}(\Gamma_{5,6})$ level to levels resulting from interaction of the $(O_h)6d(t_{2g})\Gamma_{8g}$ and $(O_h)6d(t_{2g})\Gamma_{7g}$ states, additionally split by the trigonal CF distortion, with the $5f^2(^{2S+1}L_J)$ states.

In the spectra of the U^{3+}:K_2LaX_5 (X = Cl, Br, or I) crystals, a red shift of the first f−d transitions by ∼1000 cm^{-1} was observed with respect to the first and last one in the series. In the U^{3+}:$Cs_3Lu_2Cl_9$ and U^{3+}:$Cs_3Y_2I_9$ crystals, the first f−d bands appear at a lower energy than those in the K_2LaX_5 (X = Cl or I) crystals, and with reference to the spectra of the chloride and iodide crystals, a significantly larger energy shift has been noticed which may be attributed to differences in Ln(U)−X distances. For the red shift, an increase in covalency of the U−X bonds (nephelauxetic effect) and the crystal-field strength is responsible. For shorter distances, a larger overlap of the 5f and ligand orbitals leads to larger bond covalency and the increase of the crystal-field splitting (10*Dq*) of the $5f^26d^1$ configuration also results in a red shift of the first f−d

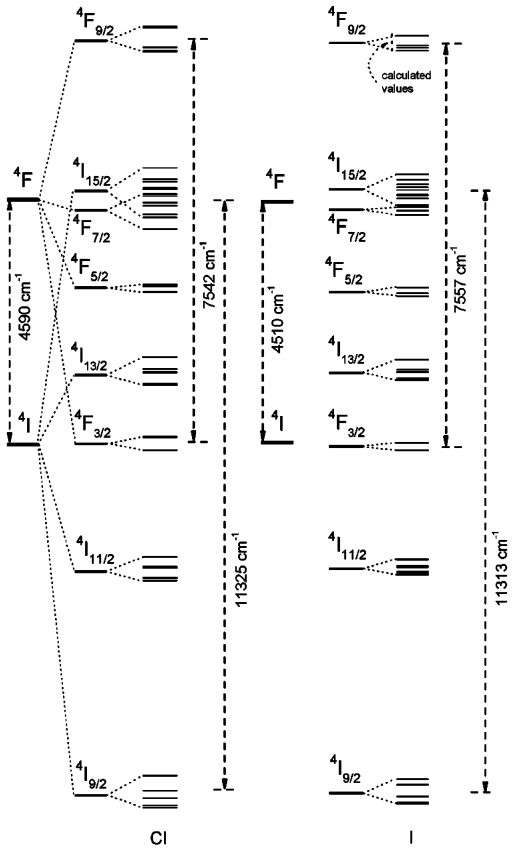

Figure 10. Schematic representation showing crystal-field energy levels resulting from the splitting of the ^4I and ^4F manifolds of U^{3+} in $Cs_3Lu_2Cl_9$ and $Cs_3Y_2I_9$ crystals.

transitions. The mean U−X distances for $Cs_3Lu_2Cl_9$ and $Cs_3Y_2I_9$ are equal to 2.57 and 2.97 Å, respectively, and are markedly shorter than those observed for K_2UCl_5 (2.84 Å) and K_2UI_5 (3.26 Å).

A similar trend has been observed also for the f−f transitions with respect to the multiplet baricenter positions (Figure 10 and Tables 1 and 2) which is exclusively caused by covalency, that is, the nephelauxetic effect. The increase in metal−ligand covalency enlarges the average distance between the valence electrons, which leads to a decrease of the Coulomb repulsion. At the same time, the delocalization of the electron density leads to a reduction of the orbital angular momentum and thus the spin−orbit coupling. The differences between the baricenters of the SL terms and SLJ multiplets may be used as a measure of the Coulomb repulsion and spin−orbit coupling, respectively. The two lowest terms for the $5f^3$ configuration are ^4I and ^4F. Unfortunately, transitions to the $^4I_{15/2}$ and $^4F_{7/2}$ multiplets are observed in a spectral range where four different multiplets ($^4S_{3/2}$ + $^4G_{5/2}$ + $^4I_{15/2}$ + $^4F_{7/2}$) overlap, resulting in a strong mixing of the eigenvectors. For that reason, those eight or four CF components for which the calculated eigenvectors exhibit the highest percentage of the $^4I_{15/2}$ or $^4F_{7/2}$ wave functions have been assigned to these multiplets, respectively, and utilized for calculation of the baricenter values. Since, in the spectrum of U^{3+}:$Cs_3Y_2I_9$, the transitions to the $^4F_{9/2}$ multiplet were obscured by f−d transitions, the calculated values of the CF components have to be taken into account for determination of the baricenter.

The Coulomb repulsion evaluated from the difference between baricenters of the ^4I and ^4F levels decreases by 1.8% with reference to U^{3+}:$Cs_3Lu_2Cl_9$ and U^{3+}:$Cs_3Y_2I_9$. In the Er^{3+}:$Cs_3M_2X_9$ type of crystals, the experimentally determined Coulomb repulsion decreases by 0.46% (ref 15). For transition-metal ions, a similar reduction of the Coulomb repulsion as well as of the spin−orbit coupling amounts to ∼15%. The significantly larger values obtained for U^{3+} as compared with rare-earth ions result from a larger extent of the 5f electrons as compared to that of 4f and a less effective shielding of the 5f electrons. Besides, the obtained values indicate a more d-electron character of the $5f^3$ configuration of U^{3+} as compared to a $4f^n$ configuration. However, the energy difference between the baricenters of the $^4F_{3/2}$ and $^4F_{9/2}$ multiplets, which is a measure of the spin−orbit coupling, does not follow the expected trend. Contrary to expectations, an increase of 0.2% is observed with reference to U^{3+}:$Cs_3Lu_2Cl_9$ and U^{3+}:$Cs_3Y_2I_9$. However, if we take into account the difference between the $^4I_{9/2}$ and $^4I_{15/2}$ multiplets, a decrease of 0.1% is noticed. Such a nonuniform trend may be a consequence of the above-mentioned, possible inaccuracy in the determination of the $^4F_{9/2}$ and $^4I_{15/2}$ multiplet baricenters.

Another significant effect is a decrease of the CF strength in the iodide crystals demonstrated by a decrease in the experimental splitting values of the SLJ multiplets. A comparison of the values for the four lowest multiplets in both crystals shows an average decrease of 33%. The smallest difference, equal to 23%, has been observed for $^4I_{9/2}$ and the largest of 46% for $^4F_{3/2}$. In the series of Er^{3+}:$Cs_3M_2X_9$ (X = Cl, Br, or I) single crystals, the observed average decrease is only slightly smaller and amounts to 28.1% (ref 15).

That a stronger CF effect is expected for the chloride than for the iodide surrounding a somewhat larger splitting of the $^2H_{9/2}$ and $^4F_{5/2}$ multiplets for U^{3+}:$Cs_3Y_2I_9$ (384 and 159 cm^{-1}) than for U^{3+}:$Cs_3Lu_2Cl_9$ (353 and 138 cm^{-1}) may be regarded to some extent as surprising. A similar behavior was observed for Er^{3+}:$Cs_3Y_2I_9$ where the total CF splitting of $^4G_{11/2}$ and $^2G_{9/2}$ exceeded the corresponding values for Er^{3+}:$Cs_3Lu_2Cl_9$ (ref 15). The authors have ascribed this irregularity to the proximity of the f−d states, which are for the iodide crystal observed at an energy as low as 30 000 cm^{-1}. A similar effect seems to account for the discrepancy observed in the spectrum of U^{3+}:$Cs_3Y_2I_9$ where the first f−d transitions are observed already at 12 000 cm^{-1}, that is, at a 3000 cm^{-1} lower energy than that for U^{3+}:$Cs_3Lu_2Cl_9$. Such irregularities were not observed between the spectra of U^{3+}:K_2LaCl_5 and U^{3+}:K_2LaI_5; however, in this case, the first f−d transitions in the iodide crystal were observed at an energy of only 1000 cm^{-1} lower than that for the chloride crystal.

It is interesting to notice that the same two multiplets for which the extent of the splitting was strongly affected by the proximity of f−d states were also the problematic multiplets for which the fitting procedure could not be well performed in the one-electron model. The discrepancy between the calculated and experimental CF splitting has been to some extent resolved by the inclusion of the CCF parameters. One of the basic mechanisms leading to the electron correlations are the configuration interactions.[31] In an analysis of U^{4+} ions, it has been also shown that one could considerably improve the rms deviation by taking into consideration the interaction between the $5f^2$ and $5f^17p^1$ configurations.[32] Therefore, it is not surprising that multiplets whose splitting strongly depends on the energy of higher configurations are mostly affected by the proximity of the f−d states, since for hosts with lower positioned $5f^26d^1$ configuration other excited configurations are also expected at adequately lower energy.

The average values of the multiplet-to-multiplet oscillator strengths are ∼20% larger for U^{3+}:$Cs_3Y_2I_9$. Depending on the specific multiplet, the differences change from 5 to 30%. The

electric-dipole forbidden f−f transitions gain their intensity due to mixing of some allowed f−d character into $5f^3$ wave functions via odd-parity CF terms. This mixing is significantly larger for U^{3+}:$Cs_3Y_2I_9$ in which the first f−d states appear at an energy as low as 12 000 cm^{-1}.

5.3. Energy Level Calculations. Crystal-field calculations of U^{3+} ions doped in isostructural host lattices, differing in the kind of ligand only, permit one to learn how experimentally observed trends are reflected by the calculated values of the CF parameters (Table 3).

The E_{av} parameter, which corresponds to the baricenter energy of the entire $5f^3$ configuration, exhibits a lower value for the iodide crystal. The experimentally observed reduction of the Coulomb repulsion, with respect to that obtained for the chloride crystal, is reflected by a reduction of the calculated F^2 and F^6 parameter values. However, that of F^4 is, contrary to expectations, somewhat larger for U^{3+}:$Cs_3Y_2I_9$ than for U^{3+}:$Cs_3Lu_2Cl_9$. This inconsistency seems to result from uncertainties in the determination of the configuration interaction parameters as well as of the T^i, M^j, and P^k parameters. For U^{3+} ions in the title crystals, they could not be properly determined due to the limited number of experimental crystal-field levels, especially to the lack of data for multiplets positioned at higher energies, for which these parameters possess the largest matrix elements. In the fitting procedures, they were kept at constant values determined for U^{3+}:$LaCl_3$ (ref 7) or by ab initio methods.[33] As a result, the inaccuracy in the determination of the values of the minor atomic interactions is compensated by the F^k parameters. The strong dependence of the F^4 parameter from the α, β, and γ configuration interaction parameters explains the deviation of the parameter values on the expected trend. Since also for Er^{3+} ions diluted in $Cs_3Lu_2Cl_9$, $Cs_3Lu_2Br_9$, and $Cs_3Y_2I_9$ single crystals the F^k parameters do not exhibit an expected steady decrease along the Cl−Br−I series of the compounds,[15] the uncertainties in the determination of some atomic parameter values, which affect the values of other parameters, for example, the Slater integrals, seem to be a more general problem encountered in the CF analysis of *nf*-electron ions in the frame of the applied parametric Hamiltonian model.

The obtained overall correlation between the calculated and experimental energy levels is as for an actinide ion fairly good. The rms deviations are about a factor of 2 larger than those for the Er^{3+} ions in the same crystals[15] and are equal to 35 and 37 cm^{-1} for U^{3+}:$Cs_3Lu_2Cl_9$ and U^{3+}:$Cs_3Y_2I_9$, respectively. In calculations performed without inclusion of CCF parameters, the rms errors are somewhat larger and amount to 50 and 48 cm^{-1} for the chloride and iodide crystals, respectively. These values are close to those obtained for U^{3+}:elpasolite systems, where the U^{3+} ions substitute for Ln^{3+} in the O_h site symmetry (57, 61, and 43 cm^{-1} for 28, 27, and 25 energy levels of U^{3+}:Cs_2LiYCl_6, U^{3+}:Cs_2NaYCl_6, and U^{3+}:Cs_2NaYBr_6, respectively),[9,10] but they are somewhat larger as compared with the reported values for U^{3+} ions doped into single crystals of a lower site symmetry of the central ion.[1,5] Similar rms errors (50 and 45 cm^{-1} in the CF and CCF models, respectively) were obtained for U^{3+}-doped $CsCdBr_3$ single crystals in C_{3v} site symmetry.[11]

The inclusion of two CCF parameters in the fitting procedure has not only improved the overall fit but has also for some multiplets corrected the ordering of the crystal-field levels. Nevertheless, the calculated order of the two lowest Stark components of the ground $^4I_{9/2}$ multiplet were still reversed, although the deviation was markedly smaller and the calculated overall splitting was closer to the experimental value in comparison with the one-electron model. A similar reordering of the two lowest components of the ground state has been observed also for Er^{3+} ions in $Cs_3Lu_2Br_9$ crystals[34] as well as for Nd^{3+} and U^{3+} ions in $CsCdBr_3$ crystals.[11,35]

In the investigated systems, as for Er^{3+}:$Cs_3Lu_2Cl_9$, Er^{3+}:$Cs_3Y_2I_9$, or U^{3+}:$CsCdBr_3$, the fourth-rank parameters dominate. The one-electron CF parameters are for U^{3+} on average a factor of 3 larger than those for Er^{3+} in the same crystals;[15] however, the differences are not regular. The largest are observed for the B_3^6 and B_6^6 parameters, which amount to −1285 and 706 cm^{-1} for U^{3+}:$Cs_3Lu_2Cl_9$ and to −974 and 995 cm^{-1} for U^{3+}:$Cs_3Y_2I_9$, while for Er^{3+} ions in the same crystals the corresponding values are equal to −185, −200, −224, and −148 cm^{-1}, respectively. Furthermore, the sign of B_6^6 for U^{3+} is the opposite to that of Er^{3+}. However, the values and signs of the B_3^6 and B_6^6 parameters correspond well to those of −990 and 656 cm^{-1}, determined for U^{3+} ions doped in the C_{3v} site of $CsCdBr_3$ single crystals.[11]

All CF parameters, with the exception of B_6^6, exhibit for the iodide smaller values than those for the chloride crystals. Similar exceptions were observed for the Er^3:$Cs_3M_2X_9$ single crystals (X = Cl, Br, or I), where the B_3^6 parameter exhibits a larger value for the iodide crystal than for the bromide and chloride crystals, and B_6^6 has a larger value for the iodide crystal than for the bromide crystal. The authors[15] have ascribed this effect to the observed irregularities in the CF splitting of multiplets centered above 25 000 cm^{-1}, where the experimental values for the iodide crystal are larger than those for the bromine and chlorine crystals. The larger splitting of the $^2H_{9/2}$ and $^4F_{5/2}$ multiplets determined for the U^{3+}:$Cs_3Y_2I_9$ crystal may account for the observed behavior of B_6^6 encountered in the determination of the proper B_6^6 parameter values and may be considered as an additional explanation of the observed discrepancy. Since this parameter reveals the largest matrix element for the $^4I_{15/2}$ multiplet, its value is strongly dependent on a proper assignment of the $^4I_{15/2}$ multiplet CF components. For U^{3+}:$Cs_3Lu_2Cl_9$, crystal transitions to this multiplet were observed in the 10 800−11 900 cm^{-1} range, where they overlap with those to the $^4G_{5/2}$ and $^4F_{7/2}$ multiplets and could not be unambiguously determined. For the U^{3+}:$Cs_3Y_2I_9$ crystals, the CF calculations have shown that due to a weaker CF the $^4F_{7/2}$ and $^4I_{15/2}$ multiplets were not mixed as well as that in the 11 000−11 800 cm^{-1} range and that the first four levels have a dominant $^4F_{7/2}$ character whereas the last eight levels should be assigned to the $^4I_{15/2}$ multiplet. However, since in this spectral range a large number of transitions is expected, the absorption lines of neighboring multiplets overlap, enabling the determination of the transition energies. Due to a different normalization, the B_q^k parameters must be multiplied by $(24)^{1/2}$ in order to attain a semiquantitative comparison between the B_q^k and G_{iq}^k parameters on a physically meaningful absolute scale. The obtained G_{10A}^4/B^4 ratios for U^{3+}:$Cs_3Lu_2Cl_9$ and U^{3+}:$Cs_3Y_2I_9$ are equal to 0.27 and 0.47, respectively, and are considerably larger than the same ratios for Er^{3+} ions, which amount to 0.15 for the chloride crystal and 0.35 for the iodide crystal.[15] For U^{3+}:$CsCdBr_3$, the appropriate ratio was equal to 0.43 (ref 11). The correlation effects are expected to be more important for the more covalent lattices as well as for 5f than for 4f electrons, which is accurately reflected by higher G_{10A}^4/B^4 ratios. On the other hand, the inclusion of CCF terms into the crystal-field Hamiltonian has a noticeable influence on the values of the one-electron B_q^k parameters for the U^{3+} ion. Thus, it seems possible that the observed improvement of the adjustment of some of the CF levels as well as that of the overall fit may not be directly related to the inclusion of CCF

interactions but results from the deficiency of the applied theoretical one-electron model for the description of the CF energy levels of the $5f^3$ configuration.

The values of the scalar crystal-field strength parameter (N_v) are equal to 4752 and 3089 cm^{-1} for U^{3+}:$Cs_3Lu_2Cl_9$ and U^{3+}:$Cs_3Y_2I_9$, respectively. They are more than 2 times larger than those of Er^{3+}:$Cs_3Lu_2Cl_9$ (2116 cm^{-1}) and Er^{3+}:$Cs_3Y_2I_9$ (1533 cm^{-1}).[15] That for U^{3+}:$CsCdBr_3$ was reported to be equal to 3479 cm^{-1} (ref 11). Obviously, the observed difference of 35% between U^{3+}:$Cs_3Lu_2Cl_9$ and U^{3+}:$Cs_3Y_2I_9$ corresponds well to the 33% average decrease in the experimental splitting values of the SLJ multiplets but does not correspond to the observed difference in the ground multiplet splitting (12%), which indicates that the latter quantity should not be treated as a representative measure of the CF strength.

For the U^{3+}:Cs_2NaYCl_6 elpasolite, where the U^{3+} ions substitute for Y^{3+} at the O_h site symmetry, the N_v parameter exhibits a value 1.4 times larger than that for U^{3+} in the C_{3v} site of the $Cs_3Lu_2Cl_9$ crystals. The stronger CF affecting U^{3+} ions in the O_h symmetry site is also reflected by the larger splitting of the ground multiplet (620 cm^{-1}). The difference in the CF strength cannot be accounted for by the difference in metal−ligand distances, since in Cs_2NaYCl_6 the $Y^{3+}-Cl^-$ distances (2.62 Å) are confined between the terminal (2.461 Å) and bridging (2.685 Å) $Lu^{3+}-Cl^-$ distances for $Cs_3Lu_2Cl_9$ and indicate that the CF symmetry is an important factor influencing the CF strength. This effect is more pronounced for U^{3+} ions than for Er^{3+} ions, where the CF strength for Er^{3+}:Cs_2NaYCl_6 (N_v = 2358 cm^{-1})[36] is only a factor of 1.12 larger than that for Er^{3+}:$Cs_3Lu_2Cl_9$ (N_v = 2098 cm^{-1}).[14]

6. Summary

Low-temperature emission and polarized absorption spectra were recorded for U^{3+} ions doped in $Cs_3Lu_2Cl_9$ and $Cs_3Y_2I_9$ single crystals. A comparison of the spectra of the title compounds with those of the U^{3+}:Cs_2MYX_6 elpasolites (M = Li or Na and X = Cl or Br) shows that the energy level structure is mainly determined by the cubic part of the CF potential. By employing free-ion, one-electron crystal-field as well as two-particle correlation crystal-field (CCF) operators with a rms deviation of 35 and 37 cm^{-1} for U^{3+}:$Cs_3Lu_2Cl_9$ and U^{3+}:$Cs_3Y_2I_9$, respectively, 57 and 39 experimental energy levels were fitted to parameters of a semiempirical Hamiltonian. The inclusion of two CCF parameters has not only improved the overall fit but has also in some multiplets corrected the sequence of the crystal-field levels.

Since the U^{3+} ions possess in both title crystals the same approximate C_{3v} local site symmetry, they were found suitable to follow the effects of variation of the halide ions on the energy levels and Hamiltonian parameter values. The first f−d transitions appear at ∼14 800 cm^{-1} for U^{3+}:$Cs_3Lu_2Cl_9$ and as low as 11 790 cm^{-1} for U^{3+}:$Cs_3Y_2I_9$. The experimental energy differences between baricenters of the ^4I and ^4F multiplets, being a measure of the Coulomb repulsion, decrease by 1.8% with reference to U^{3+}:$Cs_3Lu_2Cl_9$ and U^{3+}:$Cs_3Y_2I_9$. This value is significantly larger than that obtained for the Er^{3+}:$Cs_3M_2X_9$ (X = Cl, Br, or I) single crystals (0.46%) and is a consequence of the larger extent of 5f electrons as compared with 4f and a less effective shielding of the 5f electrons. It points to a more d-electron character of the $5f^3$ configuration of U^{3+} as compared with $4f^n$. The experimentally observed reduction of the Coulomb repulsion in the iodide crystal is reflected by a reduction of the calculated F^2 and F^6 parameter values. Contrary to expectations, the calculated value of the F^4 parameter has been found to be larger for U^{3+}:$Cs_3Y_2I_9$. The main reason for this result seems to be the uncertainties in determination of the configuration interaction parameters as well as of the T^i, M^j, and P^k atomic parameters, which could not be adjusted in the fitting procedure due to a limited set of experimental data.

The average multiplet splitting is 33% smaller in U^{3+}:$Cs_3Y_2I_9$ than in U^{3+}:$Cs_3Lu_2Cl_9$. The smallest decrease has been observed for $^4I_{9/2}$ (23%) and the largest for $^4F_{3/2}$ (46%). Remarkably, the splitting of the $^2H_{9/2}$ and $^4F_{5/2}$ multiplets is somewhat larger for the iodide crystal (384 and 159 cm^{-1}) than for the chloride crystal (353 and 138 cm^{-1}), which may be attributed to the position of f−d states, observed for U^{3+}:$Cs_3Y_2I_9$ at an energy 3000 cm^{-1} lower than that for U^{3+}:$Cs_3Lu_2Cl_9$. It is interesting to notice that these two multiplets, strongly affected by the proximity of the f−d states, were the *problematic* ones, for which the inclusion of CCF terms in the Hamiltonian was indispensable for a correct calculation of the energy level structure. This suggests that inclusion of configuration interactions between $5f^3$ and excited configurations should considerably decrease the rms deviation.

The average values of the multiplet-to-multiplet oscillator strengths are 20% larger for U^{3+}:$Cs_3Y_2I_9$. This effect may also be regarded as a consequence of the mixing of allowed f−d character into $5f^3$ wave functions via odd-parity CF terms. This mixing is obviously significantly larger for the iodide crystal, for which the first f−d states are positioned as low as 12 000 cm^{-1} above the ground state.

The 35% difference in the values of the scalar crystal-field strength parameter for U^{3+}:$Cs_3Lu_2Cl_9$ (N_v = 4752 cm^{-1}) and U^{3+}:$Cs_3Y_2I_9$ (N_v = 3089 cm^{-1}) corresponds well with the 33% average decrease in the experimental splitting values of the SLJ multiplets but does not match that of the ground multiplet splitting (12%), which indicates that the latter may not be treated as a representative measure of the CF strength. A comparison of the N_v parameters for the (C_{3v})U^{3+}:$Cs_3Lu_2Cl_9$ (C_{3v}) and (O_h)U^{3+}:Cs_2NaYCl_6 single crystals shows that the site symmetry is an important factor influencing the crystal-field strength.

Acknowledgment. This work was supported by the Polish Committee for Scientific Research within the Project No. 7TO9A080 20, which is gratefully acknowledged.

References and Notes

(1) Karbowiak, M.; Drożdżyński, J.; Murdoch, K. M.; Edelstein, N. M.; Hubert, S. *J. Chem. Phys.* **1997**, *106*, 3067.
(2) Karbowiak, M.; Drożdżyński, J. *J. Alloys Compd.* **2000**, *300*−*301*, 329.
(3) Karbowiak, M.; Gajek, Z.; Drożdżyński, J. *Chem. Phys.* **2000**, *261*, 301.
(4) Karbowiak, M.; Edelstein, N.; Gajek, Z.; Drożdżyński, J. *Spectrochim. Acta, Part A* **1998**, *54*, 2035.
(5) Karbowiak, M.; Mech, A.; Gajek, Z.; Edelstein, N.; Drożdżyński, J. *New J. Chem.* **2002**, *26*, 1651.
(6) Carnall, W. T.; Crosswhite, H. M. *ANL-89/39 report*; Argonne National Laboratory: Chicago, IL, 1989.
(7) Karbowiak, M.; Sobczyk, M.; Drożdżyński, J. *J. Chem. Phys.* **2002**, *117*, 2800.
(8) Simoni, E.; Louis, M.; Gesland, J. Y.; Hubert, S. *J. Lumin.* **1995**, *65*, 153.
(9) Karbowiak, M.; Drożdżyński, J.; Hubert, S.; Simoni, E.; Stręk, W. *J. Chem. Phys.* **1998**, *108*, 10181.
(10) Karbowiak, M.; Zych, E.; Dereń, P.; Drożdżyński, J. *Chem. Phys.* **2003**, *287*, 365.
(11) Karbowiak, M.; Drożdżyński, J.; Edelstein, N. M.; Hubert, S. *J. Phys. Chem. B* **2004**, *108*, 160.
(12) Barthem, R. B.; Buisson, R.; Cone, R. L. *J. Chem. Phys.* **1989**, *91*, 627.
(13) Andres, H. P.; Krämer, K.; Güdel, H.-U. *Phys. Rev. B* **1996**, *54*, 3830.

(14) Lüthi, S. R.; Güdel, H.-U.; Hehlen, M. P.; Quagliano, J. R. *Phys. Rev. B* **1998**, *57*, 15229.
(15) Lüthi, S. R.; Güdel, H.-U.; Hehlen, M. P. *J. Chem. Phys.* **1999**, *110*, 12033.
(16) Meyer, G. *Inorg. Synth.* **1989**, *25*, 146.
(17) Drożdżyński, J. *Polyhedron* **1988**, *7*, 167.
(18) Wybourne, B. G. *Spectroscopic Properties of Rare Earths*; Interscience: New York, 1965.
(19) Carnall, W. T.; Crosswhite, H.; Crosswhite, H. M.; Hessler, J. P.; Edelstein, N. M.; Conway, J. G.; Shalimoff, G. V.; Sarup, R. *J. Chem. Phys.* **1980**, *72*, 5089.
(20) Gschneidner, K. A., Jr.; Eyring, L., Eds. *Handbook on the Physics and Chemistry of Rare Earths*; North-Holland: Amsterdam, The Netherlands, 1982; Vol. 5, pp 482−483.
(21) Reid, M. F. *J. Chem. Phys.* **1987**, *87*, 2875.
(22) Judd, B. R. *J. Chem. Phys.* **1977**, *66*, 3163.
(23) Li, C. L.; Reid, M. F. *Phys. Rev. B* **1990**, *42*, 1903.
(24) Reid, M. F. University of Canterbury, New Zealand, private communication.
(25) Auzel, F. Malta, O. L. *J. Phys. (Paris)* **1983**, *44*, 201.
(26) Meyer, G. *Solid State Chem.* **1982**, *14*, 141.
(27) Guthrie, D. H.; Meyer, G.; Corbett, J. D. *Inorg. Chem.* **1981**, *20*, 1192.
(28) Karbowiak, M.; Drożdżyński, J. *Mol. Phys.* **2003**, *101*, 971.
(29) van Pieterson, L.; Reid, M. F.; Meijerink, A. *Phys. Rev. B* **2002**, *88*, 067405.
(30) Karbowiak, M.; Drożdżyński, J. *J. Phys. Chem. A* **2004**, *108*, 6397.
(31) Rajnak, K.; Wybourne, B. G. *J. Chem. Phys.* **1964**, *41*, 565.
(32) Faucher, M. D.; Moune, O. K.; Garcia, D.; Tanner, P. *Phys. Rev. B* **1996**, *53*, 9501.
(33) Crosswhite, H. M.; Crosswhite, H. *J. Opt. Soc. Am. B* **1984**, *1*, 246.
(34) Hehlen, M. P.; Güdel, H.-U.; Quagliano, J. R. *J. Chem. Phys.* **1994**, *101*, 10303.
(35) Quagliano, J. R.; Cockroft, N.; Gunde, K. E.; Richardson, F. S. *J. Chem. Phys.* **1996**, *105*, 9812.
(36) Richardson, F. S.; Reid, M. F.; Dallara, J. J.; Smith, R. D. *J. Chem. Phys.* **1985**, *83*, 3813.